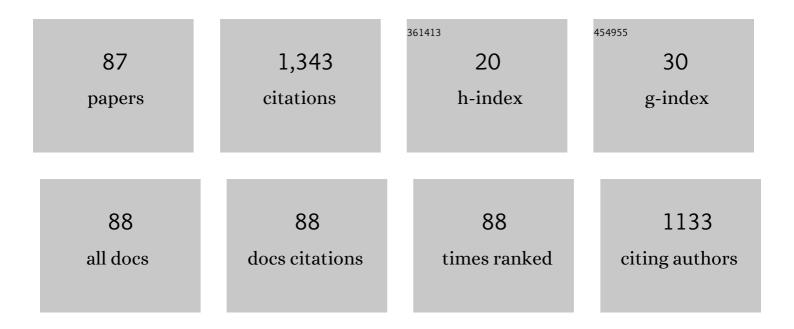
Mohammad Almasi Kashi

List of Publications by Year in descending order

Source: https://exaly.com/author-pdf/3708587/publications.pdf Version: 2024-02-01



#	Article	IF	CITATIONS
1	The effect of temperature and concentration on the self-organized pore formation in anodic alumina. Journal Physics D: Applied Physics, 2005, 38, 2396-2399.	2.8	93
2	Effect of annealing process in tuning of defects in ZnO nanorods and their application in UV photodetectors. Optik, 2016, 127, 4675-4681.	2.9	57
3	Capacitive humidity sensors based on large diameter porous alumina prepared by high current anodization. Sensors and Actuators A: Physical, 2012, 174, 69-74.	4.1	53
4	Optimum self-ordered nanopore arrays with 130–270 nm interpore distances formed by hard anodization in sulfuric/oxalic acid mixtures. Journal Physics D: Applied Physics, 2007, 40, 7032-7040.	2.8	51
5	Reversal modes in FeCoNi nanowire arrays: Correlation between magnetostatic interactions and nanowires length. Journal of Magnetism and Magnetic Materials, 2015, 378, 73-83.	2.3	44
6	Enhanced gas-sensing properties of ZnO nanorods encapsulated in an Fe-doped ZnO shell. Journal Physics D: Applied Physics, 2014, 47, 075003.	2.8	42
7	Tuning magnetic fingerprints of FeNi nanowire arrays by varying length and diameter. Current Applied Physics, 2015, 15, 819-828.	2.4	41
8	Surfactant-free synthesis and magnetic hyperthermia investigation of iron oxide (Fe3O4) nanoparticles at different reaction temperatures. Materials Chemistry and Physics, 2019, 230, 9-16.	4.0	40
9	The effect of pH and composition of sulfuric–oxalic acid mixture on the self-ordering configuration of high porosity alumina nanohole arrays. Journal Physics D: Applied Physics, 2007, 40, 4625-4630.	2.8	32
10	The influence of the ac electrodeposition conditions on the magnetic properties and microstructure of Co nanowire arrays. Journal Physics D: Applied Physics, 2006, 39, 4130-4135.	2.8	31
11	Crystallinity and magnetic properties of electrodeposited Co nanowires in porous alumina. Journal of Magnetism and Magnetic Materials, 2012, 324, 1826-1831.	2.3	31
12	The effect of magnetic layer thickness on magnetic properties of Fe/Cu multilayer nanowires. Materials Chemistry and Physics, 2014, 144, 230-234.	4.0	25
13	Fabrication of high aspect ratio Co nanowires with controlled magnetization direction using ac and pulse electrodeposition. Materials Chemistry and Physics, 2008, 112, 285-289.	4.0	23
14	Self-ordering of anodic nanoporous alumina fabricated by accelerated mild anodization method. Thin Solid Films, 2010, 518, 6767-6772.	1.8	23
15	Microstructure and magnetic properties in arrays of ac electrodeposited Fe x Ni1â^'x nanowires induced by the continuous and pulse electrodeposition. Applied Physics A: Materials Science and Processing, 2011, 102, 761-764.	2.3	23
16	Magnetostatic Interaction Investigation of CoFe Alloy Nanowires by First-Order Reversal-Curve Diagrams. IEEE Transactions on Magnetics, 2013, 49, 1167-1171.	2.1	23
17	A new approach to fabricating magnetic multilayer nanowires by modifying the ac pulse electrodeposition in a single bath. Journal Physics D: Applied Physics, 2014, 47, 355003.	2.8	23
18	Efficiency improvement in non-enzymatic H ₂ O ₂ detection induced by the simultaneous synthesis of Au and Ag nanoparticles in an RGO/Au/Fe ₃ O ₄ /Ag nanocomposite. New Journal of Chemistry, 2020, 44, 9037-9045.	2.8	23

#	Article	IF	CITATIONS
19	Irreversible evolution of angular-dependent coercivity in Fe80Ni20 nanowire arrays: Detection of a single vortex state. Journal of Magnetism and Magnetic Materials, 2016, 414, 158-167.	2.3	21
20	Optimized microstructure and magnetic properties in arrays of ac electrodeposited Co nanowires induced by the continuous and pulse electrodeposition. Journal Physics D: Applied Physics, 2007, 40, 5533-5536.	2.8	20
21	ZnO thin layer/Fe-based ribbon/ZnO thin layer sandwich structure: Introduction of a new GMI optimization method. Journal of Magnetism and Magnetic Materials, 2020, 493, 165697.	2.3	20
22	The influence of crystallinity enhancement on the magnetic properties of ac electrodeposited Fe nanowires. Applied Physics A: Materials Science and Processing, 2010, 98, 691-697.	2.3	19
23	Fabrication of single crystalline, uniaxial single domain Co nanowire arrays with high coercivity. Journal of Applied Physics, 2014, 115, 113902.	2.5	19
24	Axially adjustable magnetic properties in arrays of multilayered Ni/Cu nanowires with variable segment sizes. Superlattices and Microstructures, 2016, 95, 38-47.	3.1	18
25	Angular-dependent magnetism in Co(001) single-crystal nanowires: capturing the vortex nucleation fields. Journal of Materials Chemistry C, 2016, 4, 10664-10674.	5.5	17
26	Magnetic alloy nanowire arrays with different lengths: Insights into the crossover angle of magnetization reversal process. Journal of Magnetism and Magnetic Materials, 2017, 430, 6-15.	2.3	17
27	Controlling structural and magnetic properties in CoNi and CoNiFe nanowire arrays by fine-tuning of Fe content. Journal of Alloys and Compounds, 2018, 756, 193-201.	5.5	17
28	Electrodeposited metal nanowires as transparent conductive electrodes: Their release conditions, electrical conductivity, optical transparency and chemical stability. Materials and Design, 2018, 157, 326-336.	7.0	17
29	Super-fast fabrication of self-ordered nanoporous anodic alumina membranes by ultra-hard anodization. Electrochimica Acta, 2020, 354, 136766.	5.2	17
30	The effect of growth rate enhancement on the magnetic properties and microstructures of ac electrodeposited Co nanowires using non-symmetric reductive/oxidative voltage. Journal of Crystal Growth, 2009, 311, 4581-4586.	1.5	16
31	Electrochemical pore filling strategy for controlled growth of magnetic and metallic nanowire arrays with large area uniformity. Nanotechnology, 2016, 27, 275605.	2.6	16
32	Dual behaviors of magnetic CoxFe1â^'x (0≤≪) nanowires embedded in nanoporous with different diameters. Journal of Magnetism and Magnetic Materials, 2012, 324, 3193-3198.	2.3	15
33	Improvement in the microstructure and magnetic properties in arrays of dc pulse electrodeposited Co nanowires induced by Cu pre-plating. Journal Physics D: Applied Physics, 2013, 46, 295002.	2.8	15
34	Large scale ZnO nanorod-based UV sensor induced by optimal seed layer. Ceramics International, 2016, 42, 13421-13431.	4.8	15
35	Fixed vortex domain wall propagation in FeNi/Cu multilayered nanowire arrays driven by reversible magnetization evolution. Journal of Applied Physics, 2019, 125, .	2.5	15
36	Controlled Cu content of electrodeposited CoCu nanowires through pulse features and investigations of microstructures and magnetic properties. Applied Surface Science, 2011, 257, 9347-9350.	6.1	14

#	Article	IF	CITATIONS
37	Magnetic properties improvement through off time between pulses and annealing in pulse electrodeposited CoZn nanowires. Journal of Alloys and Compounds, 2011, 509, 8845-8849.	5.5	14
38	Developing high coercivity in large diameter cobalt nanowire arrays. Journal Physics D: Applied Physics, 2016, 49, 445001.	2.8	14
39	Stone-Wales like defects formation, stability and reactivity in black phosphorene. Materials Science and Engineering B: Solid-State Materials for Advanced Technology, 2018, 236-237, 208-216.	3.5	14
40	Selfâ€Poled Sausageâ€Like PVDF Nanowires Produced by Confined Phase Inversion as Novel Piezoelectric Nanogenerators. Advanced Materials Interfaces, 2021, 8, 2001734.	3.7	14
41	Tailoring magnetic properties in arrays of pulse-electrodeposited Co nanowires: The role of Cu additive. Journal of Magnetism and Magnetic Materials, 2016, 397, 64-72.	2.3	13
42	Tuning the optical properties of nanoporous anodic alumina photonic crystals by control of allowed voltage range via mixed acid concentration. Journal of Physics and Chemistry of Solids, 2018, 118, 221-231.	4.0	13
43	Tuning specific loss power of CoFe2O4 nanoparticles by changing surfactant concentration in a combined co-precipitation and thermal decomposition method. Ceramics International, 2022, 48, 16967-16976.	4.8	13
44	Magnetically extracted microstructural development along the length of Co nanowire arrays: The interplay between deposition frequency and magnetic coercivity. Journal of Applied Physics, 2016, 120, .	2.5	12
45	First-order-reversal-curve (FORC) diagrams of alternative chain of soft/ hard magnetic CoFe/Cu multilayer nanowires. Current Applied Physics, 2016, 16, 486-496.	2.4	12
46	Three-dimensional ZnO nanorods growth on ZnO nanorods seed layer for high responsivity UV photodetector. Applied Physics A: Materials Science and Processing, 2019, 125, 1.	2.3	12
47	Exploring the effect of Co concentration on magnetic hyperthermia properties of Co _x Fe _{3â^'x} O ₄ nanoparticles. Materials Research Express, 2020, 7, 016113.	1.6	12
48	Angular dependence of interactions in polycrystalline Co nanowire arrays. Materials Chemistry and Physics, 2015, 159, 128-138.	4.0	11
49	Hyperthermia properties of NixFe3â^'xO4 nanoparticles: a first-order reversal curve investigation. Journal of Materials Science: Materials in Electronics, 2019, 30, 21278-21287.	2.2	11
50	First order reversal curve investigation of the hard and soft magnetic phases of annealed CoFeCu nanowire arrays. Physica B: Condensed Matter, 2013, 429, 46-51.	2.7	10
51	Unraveling the roles of thermal annealing and off-time duration in magnetic properties of pulsed electrodeposited NiCu nanowire arrays. Journal of Applied Physics, 2015, 117, .	2.5	10
52	A facile method to form highly-ordered TiO ₂ nanotubes at a stable growth rate of 1000 nm min ^{â^'1} under 60 V using an organic electrolyte for improved photovoltaic properties. Journal Physics D: Applied Physics, 2017, 50, 375501.	2.8	10
53	Capturing dual behavior of the parallel coercivity in FeNi/Cu nanowire arrays by fine-tuning of segment thicknesses. Journal of Alloys and Compounds, 2020, 825, 153992.	5.5	10
54	The influence of asymmetric electrodeposition voltage on the microstructure and magnetic properties of FexCo1â`'x nanowire arrays. Journal of Crystal Growth, 2011, 327, 78-83.	1.5	9

#	Article	IF	CITATIONS
55	Electrical investigation and ultraviolet detection of ZnO nanorods encapsulated with ZnO and Fe-doped ZnO layer. Journal of Sol-Gel Science and Technology, 2014, 71, 540-548.	2.4	9
56	Magnetic phase tuning of diluted Fe-doped CuO nanoparticles through annealing temperature as characterized by first-order reversal curve analysis. Journal of Magnetism and Magnetic Materials, 2019, 482, 301-311.	2.3	9
57	Structural and magnetic tunability of Co/Cu multilayer nanowires induced by electrolyte acidity and spacer layer thickness. Journal of Alloys and Compounds, 2020, 820, 153087.	5.5	9
58	Structure and magnetic properties of CoxCu1â^'x nanowires in self-assembled arrays. Journal of Alloys and Compounds, 2012, 540, 133-136.	5.5	8
59	Template-based electrodeposited nonmagnetic and magnetic metal nanowire arrays as building blocks of future nanoscale applications. Journal Physics D: Applied Physics, 2022, 55, 233002.	2.8	8
60	Deciphering magnetic hyperthermia properties of compositionally and morphologically modulated FeNi nanoparticles using first-order reversal curve analysis. Nanotechnology, 2019, 30, 025707.	2.6	7
61	High Chemical and Thermal Stability of Ag Nanowireâ€Based Transparent Conductive Electrodes Induced by Electroless Ag Nanoparticle Decoration. Physica Status Solidi (A) Applications and Materials Science, 2020, 217, 1900957.	1.8	7
62	Detailed magnetic characteristics of cobalt ferrite (CoxFe3â^'xO4) nanoparticles synthesized in the presence of PVP surfactant. Applied Physics A: Materials Science and Processing, 2020, 126, 1.	2.3	6
63	In situ precipitation synthesis of FeNi/ZnO nanocomposites with high microwave absorption properties. Materials Chemistry and Physics, 2021, 266, 124508.	4.0	6
64	Pulse electrodeposition of Co1â^'xZnx nanowire arrays: Magnetic improvement through electrolyte concentration, off-time between pulses and annealing. Journal of Magnetism and Magnetic Materials, 2012, 324, 3944-3950.	2.3	5
65	FORC investigation of as-deposited and annealed CoZn alloy nanowires. Physica B: Condensed Matter, 2014, 452, 124-130.	2.7	5
66	The effect of deposition parameters on the magnetic behavior of CoFe/Cu multilayer nanowires. European Physical Journal Plus, 2015, 130, 1.	2.6	5
67	Small-diameter magnetic and metallic nanowire arrays grown in anodic porous alumina templates anodized in selenic acid. Applied Physics A: Materials Science and Processing, 2021, 127, 1.	2.3	5
68	Tunable magnetocrystalline easy axis in cobalt nanowire arrays by zinc additive. Materials Science and Engineering B: Solid-State Materials for Advanced Technology, 2016, 207, 18-25.	3.5	4
69	Analysis of structural and UV photodetecting properties of ZnO nanorod arrays grown on rotating substrate. Journal of Sol-Gel Science and Technology, 2018, 85, 458-469.	2.4	4
70	Study on magnetic properties of NiFe/Cu multisegmented nanowire arrays with different Cu thicknesses via FORC analysis: coercivity, interaction, magnetic reversibility. Journal of Materials Science: Materials in Electronics, 2018, 29, 18771-18780.	2.2	4
71	Probing the interplay between reversibility and magnetostatic interactions within arrays of multisegmented nanowires. Journal of Materials Science, 2018, 53, 14629-14644.	3.7	4
72	Etching of ZnO nanorods by ZnO nanoparticles and adjustment of morphological and UV photodetection properties. Journal of Sol-Gel Science and Technology, 2020, 95, 109-118.	2.4	4

#	Article	IF	CITATIONS
73	Self-ordered Porous Anodic Alumina Templates by a Combinatory Anodization Technique in Oxalic and Selenic Acids. Journal of Electronic Materials, 2021, 50, 4787-4796.	2.2	4
74	Synthesis and characterization of ultrafine γ-Al2O3:Cr nanoparticles and their performance in antibacterial activity. Journal of Sol-Gel Science and Technology, 2021, 99, 178-187.	2.4	4
75	Room temperature CPP-giant magnetoresistance in Ni/Cu multilayered nanowires. Journal of Alloys and Compounds, 2022, 894, 162286.	5.5	4
76	The role of barrier layer temperature in the formation of long and small-diameter TiO2 nanotube arrays. Journal of Porous Materials, 2020, 27, 1613-1621.	2.6	3
77	The influence of point defects on Na diffusion in black phosphorene: First principles study. Journal of Physics and Chemistry of Solids, 2020, 143, 109432.	4.0	3
78	Self-Ordered Nanopore Arrays with 300–400 nm Interpore Distances Formed by High Field Accelerated Mild Anodization. Japanese Journal of Applied Physics, 2011, 50, 035203.	1.5	2
79	Effect of AC Electrodeposition Conditions on Microstructure and Magnetic Properties of Co _x Ni _{1-x} Nanowire Arrays Embedded in Anodic Aluminum Oxide Template. Japanese Journal of Applied Physics, 2012, 51, 025003.	1.5	2
80	The role of different initial rest times on synthesized buffer layer and UV sensing of ZnO nanorods grown on rotational substrate. Journal of Materials Science: Materials in Electronics, 2018, 29, 8303-8312.	2.2	2
81	Developing Cu pore-filling percentage in hard anodized anodic aluminum oxide templates with large diameters. Materials Chemistry and Physics, 2021, 260, 124109.	4.0	2
82	Enhancement and recovery of magnetic exchange coupling properties in SrFe11AlO19@NiFe2O4 core-shell structure by multiple TiO2 and SiO2 nanolayer shells. Journal of Magnetism and Magnetic Materials, 2021, 530, 167932.	2.3	2
83	Angular-dependent magnetic properties of chemically synthesized single crystalline Co nanowires. Materials Chemistry and Physics, 2022, 281, 125807.	4.0	2
84	Magnetization reversal properties and magnetostatic interactions of disk to rod-shaped FeNi layers separated by ultra-thin Cu layers. Nanotechnology, 2022, 33, 365701.	2.6	2
85	Self-ordered nanopore arrays through hard anodization assisted by anode temperature ramp. Applied Physics A: Materials Science and Processing, 2016, 122, 1.	2.3	1
86	Self-Ordered Nanopore Arrays with 300–400 nm Interpore Distances Formed by High Field Accelerated Mild Anodization. Japanese Journal of Applied Physics, 2011, 50, 035203.	1.5	1
87	Effect of AC Electrodeposition Conditions on Microstructure and Magnetic Properties of CoxNi1-xNanowire Arrays Embedded in Anodic Aluminum Oxide Template. Japanese Journal of Applied Physics. 2012, 51, 025003.	1.5	0